MANUFACTURE A BEND-TWIST COUPLED BEAM

Cheng Huat Ong , Julie Wang, and Stephen W. Tsai

Department of Aeronautics and Astronautics, Stanford University
Stanford, CA 94305-4035, USA.

SUMMARY: This paper describes a manufacturing process to fabricate a bend-twist coupled beam and presents the tensile test results of three joint designs related to the anisotropic beam fabrication. To make a successful anisotropic (bend-twist coupled) beam, the joint design at the seam, where two clamshells which have symmetric lay-up meet, is very critical. The investigation looked into the advantages and disadvantages of three joint designs: butt joint, overlap joint and stagger-overlap joint. Among these designs, a stagger-overlap joint not only provides the smoothest skin thickness distribution but also has the highest joint strength retention. The retention strength at the joint depends on the ply orientation, the composition of a laminate, and the stacking sequence within it. One of the findings from the experiments is that the joint strength of a laminate which composes of 0°-plies and angle-plies and has the angle-plies at the outer layers is stronger than that of a laminate with the same plies composition but having 0°-plies at the outer layers.

KEYWORDS: bend-twist coupled, stagger-overlap joint, joint strength.

INTRODUCTION

A composite design that exhibits various degrees of anisotropy has tremendous advantages not seen in an orthotropic composite structure. The benefits are seen in a fixed wing, a helicopter blade or a wind turbine blade design.

One of the applications of aeroelastic tailoring is the use of a bend-twist coupled composite wing to prevent divergence of the forward swept wing [1]. Weisshaar [1] also highlighted other potential benefits; such as load relief, vibration control and increase of lift coefficients; for a bend-twist coupled wing.

Smith & Chopra [2] summarized that composite designs that exhibit various couplings appear to have great potential for use in helicopter blades and tilt-rotor blades to reduce vibration, enhance aeroelastic stability, and improve aerodynamic efficiency.

The application of elastic (or aeroelastic) tailoring can also be found in wind turbine applications. Karaolis [3, 4] demonstrates that the concept of anisotropy lay-ups in blade skin to achieve different types of twist coupling for wind turbine applications. Kooijman [5] investigated the optimum bend-twist flexibility distribution of a rotor blade to improve rotor blade design. Lobitz & Veers [6] indicates that the flutter and divergence speeds of a

Combined Experimental Blade (CEB) are a function of the strength of the bend-twist coupling.

There are essential issues need to be resolved before the benefits of an aeroelastic-tailoring blade can be actually realized. One of the issues is the amount or the degree of coupling that can be achieved from composite materials. This issue has been addressed in reference [7]. Another critical issue is the ability to manufacture a bend-twist-coupled blade. To produce the bend-twist coupling characteristics, the fiber lay-ups at the top and bottom skin of a blade shall be symmetric in relation to the middle plane of the blade. Such lay-ups cause fibers discontinuing at the seam. The joint design at the seam is the major consideration in fabricating a truly anisotropic beam. There are three joint designs (see Figure 1): butt joint, overlap joint and stagger-overlap joint; can be employed at the seam.

The paper here describes a manufacturing process for fabricating a bend-twist-coupled beam (D-spar) with a staggered overlap joint at the seam. The paper then presents the results of the strength test for the three joint designs. The effects of the types of joints, the overlap length, the laminate lay-up, and the stacking sequence on the joint strength have been investigated.

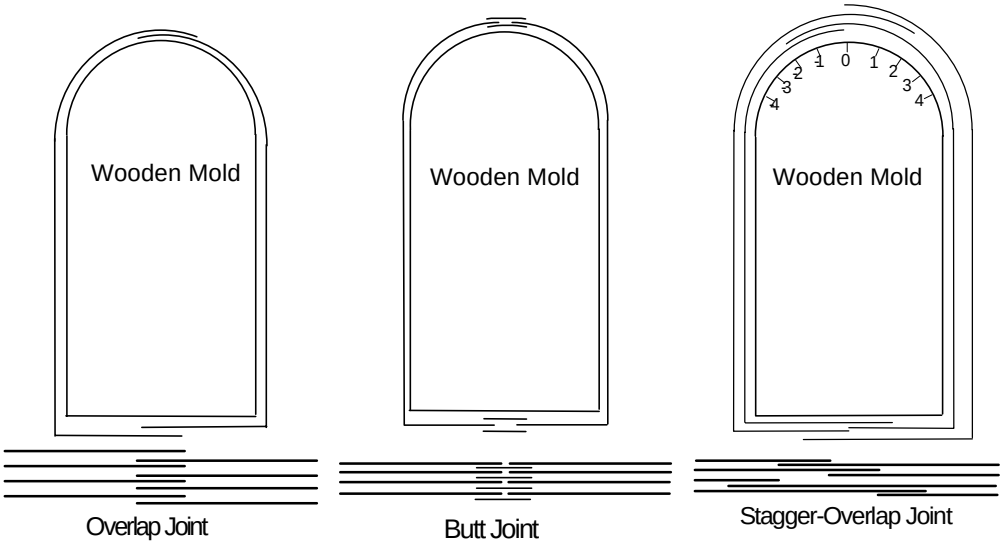

Fig. 1: Three Joint Designs

ANISOTROPIC BEAM FABRICATION

Reference [7] gives detail description on design consideration and static testing of a bend-twist coupled beam (D-spar); manufacturing of a D-spar is also briefly mentioned. A brief summary on designing a bend-twist coupled D-spar is given below.

The basic dimension of the D-spar is 182.9 cm (6 feet) long, 15.2 cm (6 inches) wide, and 7.6 cm (3 inches) high. The cross-section dimensions are shown in Figure 2.

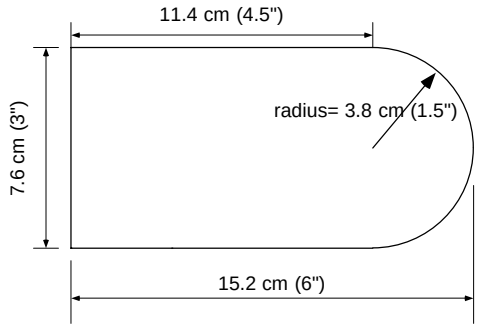

Fig. 2: D-spar Dimensions

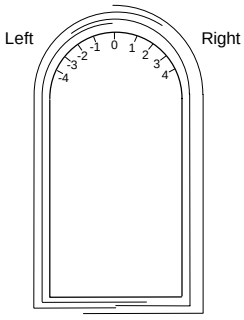

Fig. 3: End-Markings on the Wooden Mold for Lay-up

Three bend-twist coupled D-spars have been designed to achieve the objective of having maximun bend-twist coupling and fulfilling desirable structural properties. The skin laminate lay-ups of these D-spars are,

a. $[60_1/20_{24}/60_1]_T$ for all-carbon D-spar,
b. $[-60_1/25_{60}/-60_1]_T$ for all-glass D-spar, and
c. $[70_1(g)/20_9(c)/20_8(g)/20_9(c)/70_1(g)]_T$ for the hybrid D-spar (where 'c' denotes carbon fibers and 'g' refers to glass fibers).

Two D-spars, the all-carbon and the hybrid D-spar, have been fabricated using the bladder process. The bladder process uses an inflatable mandrel (nylon plastics bag was used for D-spar fabrication) to pressurise the laminate surface. The inflatable mandrel is inflated from an external source and the pressure is transferred to the laminate surface. The laminate surface is pressed against female mold to give smooth surface finish. The subsequent paragraphs describe the process of fabricating a bend-twist coupled D-spar.

A wooden mold, sized close to the internal dimensions of the D-spar, has been made and used for the lay-up process. At both ends of the wodden mold, markings are placed along the edge of the circular section (see Figure 3). One marking division is about one cm (0.4"). The markings are to facilitate the formation of the stagger-overlap joint. A sheet of release film is then placed around the wooden mold to ease the removal of the wooden mold at a later stage. The prepregs are cut the right width size (see Table 1 & 2) and the cut prepregs are then laid onto the wooden mold according to the laminate schedule as given in Table 1 & 2.

Table 1: Lay-up Laminate Schedule for the All-Carbon D-spar (see also Figure 3)

Sequence No:	Layers of Prepregs	Ply Orientation (°)	Type of Material	Prepregs Width (cm)	Lay from Wooden Mold's Marking	
					Left-Side	Right-Side
1	1	60	Carbon	22	1	-1
2	6	20	Carbon	22.2	0	-2
3	6	20	Carbon	22.7	2	0
4	6	20	Carbon	23.1	-2	-4
5	6	20	Carbon	23.7	4	2
6	1	60	Carbon	23.8	1	-1

Table 2: Lay-up Laminate Schedule for the Hybrid D-spar (see also Figure 3)

Sequence No:	Layers of Prepregs	Ply Orientation (°)	Type of Material	Prepregs Width (cm)	Lay from Wooden Mold's Marking	
					Left-Side	Right-Side
1	1	70	Glass	22	0	-2
2	8	20	Carbon	22.1	0	-2
3	4	20	Glass	22.5	-2	-4
4	2	20	Carbon	22.7	1	-1
5	4	20	Glass	22.8	4	2
6	8	20	Carbon	23.0	2	0
7	1	70	Glass	23.4	2	0

After the lay-up is completed, the mold, enclosed by the uncured laminate, is transferred to the female tooling (see Figure 4). The female tooling consists of one 'U' shape plate, one base plate, and two flat plates. Fasteners are placed along the lengthwise direction for the assembly. Before the transfer, all inner surfaces of the female tooling are cleaned and wetted with release agent. The uncured D-spar is placed inside the 'U' plate and the wooden mold is then removed from the uncured D-spar. An inflatable nylon bag is inserted into the hollow section of the D-spar before the assembly of female tooling. The inflatable bag has a nozzle attached at one end and is sealed tight at the other end.

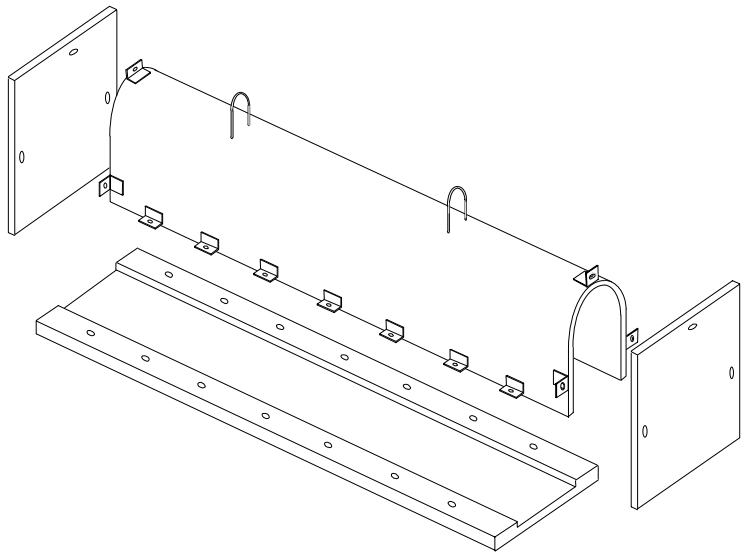

Fig. 4: D-spar Female Tooling

The whole assembly is then transferred to an oven for curing. The nozzle is connected to an external compressor unit. The D-spar is pressurized to 85-90 MPa. and cured according to the curing cycle (see Figure 5). The two cured D-spars, the hybrid D-spar and the all-carbon D-spar, are shown in Figure 6.

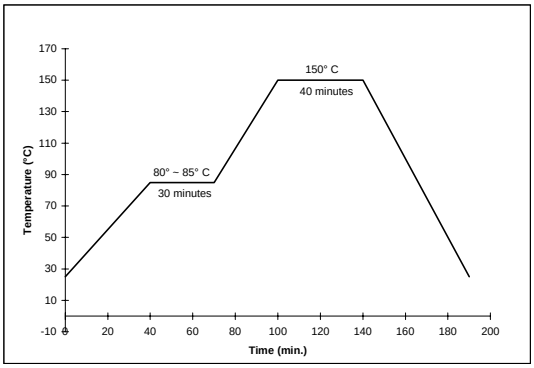

Fig: 5: D-spar Curing Cycle


Fig: 6: Hybrid and All-Carbon D-spar

Joint Designs & Strength Tests

One critical area in D-spar (or any bend-twist coupled blade) fabrication is the joint design at the seam of the two symmetric clamshells. Three types of joints have been considered: butt joint, overlap joint, and stagger-overlap joint. Both butt joint and overlap joint have distinct disadvantages on thickness distribution in the region between the main skin and the joint area. The thickness at the joint area for the joint designs is double as compared to the laminate skin. On the other hand, the stagger-overlap joint design yields better thickness distribution at that region. For example, the number of plies near the mid-plane of the fabricated D-spar is 39 layers instead of 56 layers if either the butt joint design or the overlap joint design is used. Farther away from the mid-plane, the number reduces to 28 layers, which is the total number of layers at the top and bottom skins, at a step of 3-4 ply-drop.

To test the joint strength, coupons specimen are used. Each coupon specimen has a gauge length of 12.7 cm (5") and average width of 2.54 cm (1"). The joint (either one of the three joint designs) is made at the mid-portion of a coupon. The test procedure is according to ASTM-D3039 [8]. The complete test matrix is given in Table 3.

Table 3: Tensile Strength Test Configuration

Types of Joints	Configuration Code
Baseline (Base) (without Joint)	Base-$[0_4]_S$, Base-$[\pm30_2]_S$, Base-$[\pm45_2]_S$, Base-$[0_2/\pm30]_S$; Base-$[0_2/\pm45]_S$
Stagger-overlap Joint (SO)	SO-8-0-$[0_4]_S$, SO-8-1/4-$[0_4]_S$, SO-8-1/2-$[0_4]_S$, SO-8-3/4-$[0_4]_S$; SO-8-1-$[0_4]_S$, SO-12-1/2-$[0_6]_S$, SO-16-1/2-$[0_8]_S$, SO-16-1-$[0_8]_S$; SO-8-1/2-$[\pm30_2]_S$, SO-8-1/2-$[\pm45_2]_S$, SO-8-1/2-$[\pm45/0_2]_S$; SO-8-1/2-$[0_2/\pm45]_S$, SO-8-1/2-$[\pm30/0_2]_S$, SO-8-1/2-$[0_2/\pm30]_S$
Overlap Joint (O)	O-8-1/2-$[0_4]_S$, O-8-1/2-$[\pm30_2]_S$, O-8-1/2-$[\pm45_2]_S$, O-8-1/2-$[\pm45/0_2]_S$; O-8-1/2-$[\pm30/0_2]_S$
Butt Joint (B)	B-8-1/2-$[0_4]_S$, B-8-1/2-$[\pm45_2]_S$

The definitions of alphanumeric code for each joint configuration are given below.

a. The first set of alphanumeric code represents the type of joins: butt joint (B), overlap joint (O) and stagger-overlap joint (SO).
b. The second set of alphanumeric code represents the number of ply layers.
c. The third set of alphanumeric code represents the overlap length in inches for various types of joints.
d. The last one represents the laminate lay-up.

As we are interested in the strength retention, it is more appropriate to normalize the results by the corresponding baseline (without any joint) strength. The tensile strength of each

baseline configuration is given in Table 4. And the test results of the joint retention strength are summarized in subsequent paragraphs.

Table 4: Tensile Strengths of the Baseline Configurations

Configuration Code	Ultimate Strength, MPa (ksi)
Base-$[0_4]_S$	1499 (217.3)
Base-$[\pm 30_2]_S$	341 (49.5)
Base-$[\pm 45_2]_S$	123 (17.8)
Base-$[0_2/\pm 30]_S$	872 (126.4)
Base-$[0_2/\pm 45]_S$	874 (126.7)

Table 5: Retention Strength for the Three Joints

Configuration Code	$\sigma_U/\sigma_{U(baseline)}$
SO-8-1/2-$[0_4]_S$	0.62
B-8-1/2-$[0_4]_S$	0.52
O-8-1/2-$[0_4]_S$	0.46
SO-8-1/2-$[\pm 45_2]_S$	1.21
B-8-1/2-$[\pm 45_2]_S$	1.23
O-8-1/2-$[\pm 45_2]_S$	1.12
SO-8-1/2-$[\pm 30_2]_S$	1.07
O-8-1/2-$[\pm 30_2]_S$	0.97

Three Joint Designs: Table 5 shows the strength retention for three types of joints at three laminate lay-up configurations. The results indicate that the stagger-overlap joint has the highest strength retention for 0°-ply laminate. For the angle-ply laminates, the failure is not at the joint area but at the base laminate. Therefore, it is deduced that the joints are stronger than the base laminate.

Overlap Length: The effect of overlap length on the joint strength has been studied. The investigation only focused on the 0°-ply laminate with stagger-overlap joint. The joint retention strength, as indicated in Figure 7, increases as the normalized overlap length (l/t) and the number of repeated stacking cycles (see Figure 8 for definition) increase.

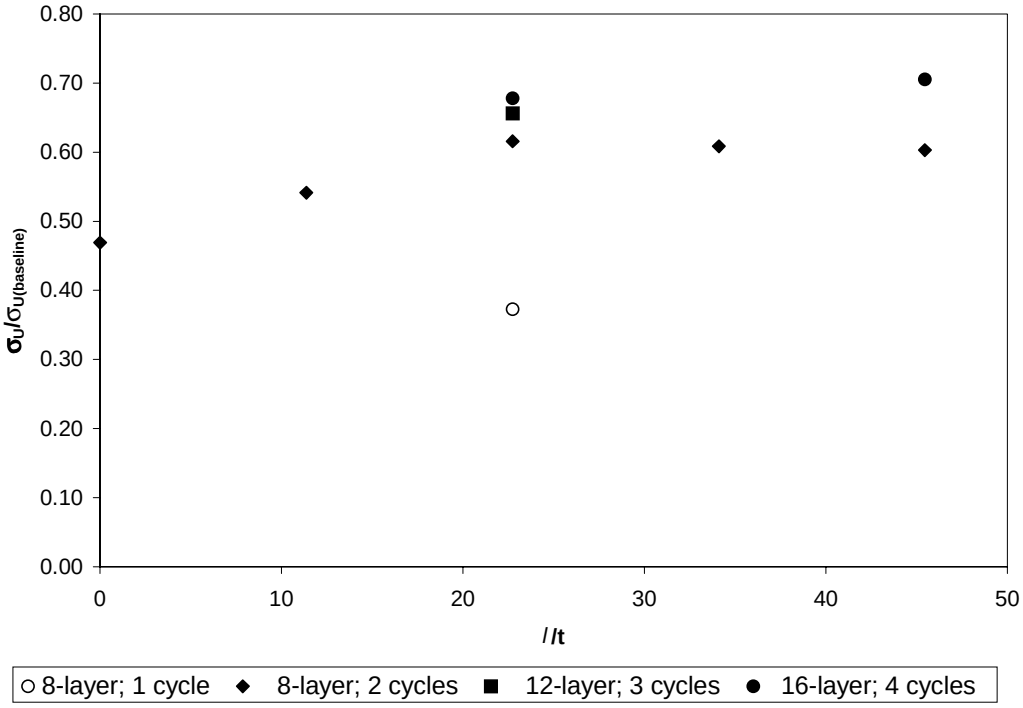

Fig: 7 Retention Strength of a Stagger-Overlap Joint with 0°-ply Lay-up

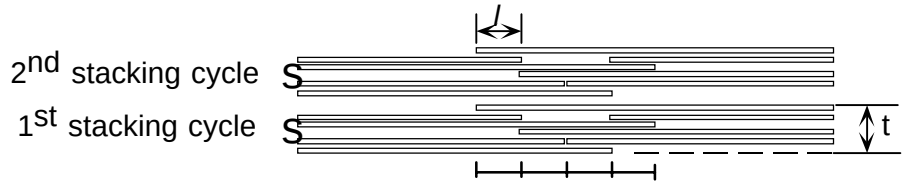

Stagger-Overlap Joint

Fig: 8 Definition of Parameters for Stagger-Overlap Joint

Laminate Composition: Table 6 shows the joint strengths of the overlap joint and stagger-lap joint for a laminate composes of 0°-ply and angle-ply. The results indicate that the addition of angle-ply into the 0°-ply increases the overall joint strength as compared to that of total 0°-ply laminate.

Stacking Sequence: Table 7 shows the effect of stacking sequence for a laminate, consists of 0°-ply and angle-ply, for the overlap joint and stager-overlap joint. The joint strengths are reduced by about 20% if the 0°-ply layers are placed at the outer layers.

Table 6: Retention Strength for Laminate (Combination of 0°-ply and Angle-ply)

Configuration Code	$\sigma_U/\sigma_{U(baseline)}$
SO-8-1/2-$[\pm45/0_2]_S$	0.78
O-8-1/2-$[\pm45/0_2]_S$	0.74
SO-8-1/2-$[\pm30/0_2]_S$	0.86
O-8-1/2-$[\pm30/0_2]_S$	0.80

Table 7: Stacking Sequence Affecting the Retention Strength

Configuration Code	$\sigma_U/\sigma_{U(baseline)}$
SO-8-1/2-$[\pm45/0_2]_S$	0.78
SO-8-1/2-$[0_2/\pm45]_S$	0.54
SO-8-1/2-$[\pm30/0_2]_S$	0.86
SO-8-1/2-$[0_2/\pm30]_S$	0.62

CONCLUSIONS

A truly anisotropic (bend-twist coupled) beam is successfully manufactured with a stagger-overlap joint design at the seam. The stagger-overlap joint design not only smoothly spreads out the thickness but also has the highest retention strength among the three joint designs. The retention strengths of the joints depend on the laminate composition and the stacking sequence. The 0°-ply laminate with stagger-overlap joint retains about 60% the corresponding tensile failure strength; the angle-ply laminate fails at the base laminate not at the joint region. To have a stronger joint strength for a laminate with combination of 0°-ply and angle-ply, the angle-ply layers should be placed at the outer layers.

ACKNOWLEDGEMENTS

This research work was supported by the Sandia National Laboratories, Technical Monitor Dr Paul S. Veers, Contract No. BB-6066. The authors would also like to thank the staffs and researchers from Materials Research Laboratories/ Industrial Technology Research Institute (Taiwan) for their support and assistance in the fabrication and static testing of D-spars.

REFERENCES

1. T. Weisshaar, "Aeroelastic Tailoring - Creative Uses of Unusual Materials," AIAA Paper No. 87-0976-CP, 1987.

2. E. C. Smith and I. Chopra, "Formulation and Evaluation of an Analytical Model for Composite Box-Beams," AIAA-90-0962-CP, 1990.

3. N.M. Karaolis, P.J. Mussgrove and G. Jeronimidis, "Active and Passive Aerodynamic Power Control Using Asymmetric Fiber Reinforced Laminates for Wind Turbine Blades," Proc. *10th British Wind Energy Conf.*, D.J. Milbrow Ed., London, March 22-24, 1988.

4. N.M. Karaolis, G. Jeronimidis and P.J. Mussgrove, "Composite Wind Turbine Blades: Coupling Effects and Rotor Aerodynamic Performance," Proc., *EWEC'89*, European Wing Energy Conf., Glasgow, Scotland, 1989.

5. H.J.T. Koijman, "Bending-Torsion Coupling of a Wind Turbine Rotor Blade," ECN-I-96-060, December 1996.

6. D.L. Lobitz and P.S. Veers, "Aeroelastic Behavior of Twist-Coupled HAWT Blades," AIAA-98-0029, Proc. *1998 ASME Wind Energy Symposium* held at 36th AIAA Aerospace Sciences Meeting and Exhibition, Reno, NV, Jan. 12-15, 1998.

7. C.H. Ong, J. Wang and S. Tsai, "Design, Manufacture and Testing of a Bend-Twist Coupled D-spar," AIAA-99-0025, Proc. *1999ASME Wind Energy Symposium* held at 37th AIAA Aerospace Sciences Meeting and Exhibition, Reno, NV, Jan. 11-14, 1999.

8. "Standard Test Method for Tensile Properties of Fiber-Resin Composites," ASTM-D3039.